Weather Classification Using Passive Acoustic Drifters

JEFFREY A. NYSTUEN

Applied Physics Laboratory, University of Washington, Seattle, Washington

HARRY D. SELSOR

Tactical Oceanography Warfare Support Program Office, Naval Research Laboratory—Detachment, Stennis Space Center, Mississippi

(Manuscript received 26 February 1996, in final form 16 August 1996)

ABSTRACT

Weather observations are needed in remote oceanic regions to support numerical weather forecast models, to provide surface truth for satellite sensors, and to help understand global weather patterns. An acoustic mini-drifting buoy using no moving parts has been designed to meet operational naval demands for real-time monitoring of upper-ocean air–sea interface processes. This buoy is an air-deployable, standard sonobuoy-sized buoy that uses an Argos satellite link to transmit data to users. Interpretation of the ambient sound field allows classification of weather into five categories: wind, wind and drizzle, rain, high seas, and shipping contaminated. Quantitative estimates of wind speed are shown to be in agreement with the Special Sensor Microwave/Imager satellite sensor. Rainfall detection is confirmed and rainfall rate quantified using an acoustic rainfall-rate algorithm. Atmospheric pressure, air and sea temperature, and ambient sound levels are measured directly.

1. Introduction

Physical processes at the air–sea interface, in particular wave breaking and precipitation, play a central role in the exchange of heat, momentum, water, and gas between the ocean and the atmosphere. Accurate measurements of these processes is very difficult, especially in remote oceanic regions, where conditions are often inhospitable. In addition, while satellite sensors provide global coverage, surface verification of the quantities being measured are needed. Fortunately, wave breaking (usually wind generated) and precipitation (both drizzle and heavier rain) are the principal sources of high-frequency (over 500 Hz) underwater sound in the ocean. Furthermore, extensive near-surface bubble clouds modify these sound sources, allowing detection of the bubble clouds (high seas). The sensor used to make underwater sound field measurements is robust, compact, and has no moving parts. Expendable autonomous drifting buoys using hydrophones have recently been developed to provide real-time measurements of upper-ocean conditions (Selsor 1993). Interpretation of the underwater ambient sound field is used to detect air–sea weather conditions and quantify wind speed or rainfall rate. Conventional measurements of air–sea temperature, atmospheric pressure, and ambient noise levels are also available.

2. Background: Underwater sound generation by wind and rain

Mechanical devices designed to measure wind and precipitation are difficult to deploy in the oceanic environment because of fouling, platform stability, and exposure problems. Fortunately, these same processes generate sound underwater and this sound can be used as a signal to quantitatively measure wind speed and rainfall rate. Figure 1 presents generic underwater spectral acoustic signatures of various air–sea interaction phenomena. Because each of these phenomena possess different acoustic signatures, Shaw et al. (1978) proposed making geophysical measurements of wind speed (stress) and precipitation using passive underwater ambient noise sensors.

Wind speed has been associated with underwater sound levels since Knudsen et al. (1948). Evans et al. (1984) and Lemon et al. (1984) documented the ability to measure wind speed using ambient sound. The source of sound generation by wind is breaking wind waves (Farmer and Vagle 1988). At high frequencies (above 500 Hz), acoustic radiation from newly created individual bubbles within the whitecap can be used to explain the observed spectral signature of wind (Medwin and Beaky 1989). At lower frequencies, the collective oscillation of bubble clouds has been observed to radiate sound (Loewen and Melville 1994). Vagle et al. (1990)

Corresponding author address: Dr. Jeffrey A. Nystuen, Applied Physics Laboratory, University of Washington, 1013 NE 40th Street, Seattle, WA 98105.
E-mail: nystuen@apl.washington.edu

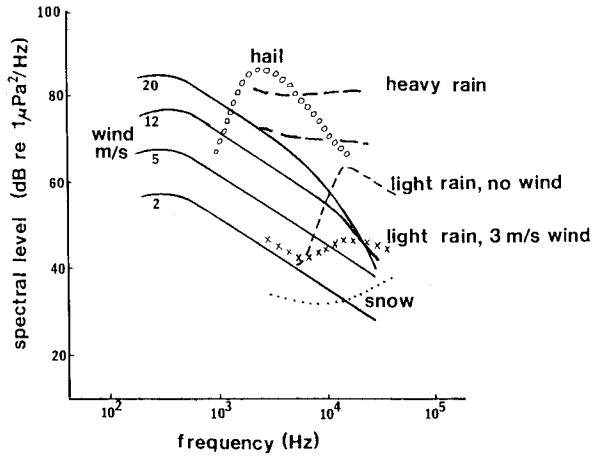

FIG. 1. Generic underwater sound spectra for different air–sea physical processes. The ''wind'' curves were first reported by Knudsen et al. (1948); Wenz (1962) gives a review. The high-frequency roll-off of the wind curves is attributed to subsurface bubbles (Farmer and Lemon 1984). The ''light rain'' spectra are reported in Nystuen and Farmer (1987). The ''heavy rain'' spectra are from Nystuen et al. (1993). The ''hail'' and ''snow'' spectra are from Scrimger et al. (1987).

proposed a generalized algorithm for inferring wind speed from ambient sound measurements. This algorithm includes flags for precipitation and shipping, two other dominant (but fortunately intermittent) noise sources in the frequency bands being used to measure wind (1–15 kHz).

The Vagle et al. (1990) algorithm was evaluated by Dailey (1991). Data from two prototype acoustic drifters deployed off of the California coast were compared with wind speed fields observed using the Defense Meteorological Satellite Program (DMSP) Special Sensor Microwave/Imager (SSM/I) (Goodberlet et al. 1989). Good agreement between the acoustical and satellite measurements was observed. The correlation coefficient r was 0.8 and the slope of the linear regression was near 1 (Dailey 1991). The scatter observed was similar to the scatter observed during comparison of wind speed from buoys and SSM/I wind speed estimates (Goodberlet et al. 1989).

Rain is another dominant source of underwater sound (Heindsman et al. 1955). Laboratory studies have identified the sound production mechanisms associated with raindrop splashes (Franz 1959; Pumphrey et al. 1989; Medwin et al. 1992; Nystuen and Medwin 1995). There are two raindrop sizes that are important for underwater sound generation. These are ''small,'' 0.8–1.1-mm-diameter, and ''large,'' 2.2–4.6-mm-diameter raindrops. These two drop sizes regularly trap bubbles, extremely effective sound generators, underwater during the raindrop splash. Because of different size distributions of the bubbles created by these two drop sizes, different underwater sound spectra are generated by light rain (containing only small drops) and heavy rain (containing both small and large drops).

Wind has been shown to strongly affect the sound produced by light rain (Nystuen and Farmer 1987; Nystuen 1993) and consequently quantitative estimates of rainfall rate from light rain without knowledge of the wind conditions are unlikely. On the other hand, detection of light rain is possible, even in high sea states (Nystuen and Farmer 1989). In the case of heavy rain, the sound produced is independent of wind speed, at least for wind speeds less than 10 m s^{-1} (Nystuen et al. 1993) and so detection and quantification of rainfall rate is possible. Furthermore, since each raindrop size produces sound with unique spectral characteristics, the sound spectrum can be inverted to measure raindrop size distribution (Nystuen 1996). Dailey (1991) verified detection of rainfall from acoustic drifters at times when SSM/I rainfall-rate fields indicated rainfall over the buoys.

One additional measurement directly related to gas exchange is also possible from the sound field. Farmer and Lemon (1984) reported that for wind speeds above 10 m s^{-1}, relatively low sound levels are observed at frequencies above 10 kHz (when compared to 4 kHz). They suggest that this is due to attenuation of surface generated sound passing through ambient bubble clouds. Because acoustical attenuation by bubbles is frequency dependent, bubble populations can be estimated by measuring the apparent attenuation (Farmer and Lemon 1984; Nystuen and Farmer 1989). These bubbles affect sound speed and acoustical reverberation at the ocean surface and consequently modify sound propagation in the surface sound duct. Furthermore, they are an indication of turbulent mixing in the near surface layer.

3. Drifting buoy description

The naval designation for the drifting buoys used in this study is AN/WSQ-6 series, model XAN-2, ambient noise sensor (ANS) drifters. These buoys fit inside a standard A-sized sonobuoy canister (Fig. 2). They are certified to be air deployed using a standard sonobuoy chute from aircraft. As the canister leaves the airplane, the end cap is pulled off and a parachute deploys. Upon

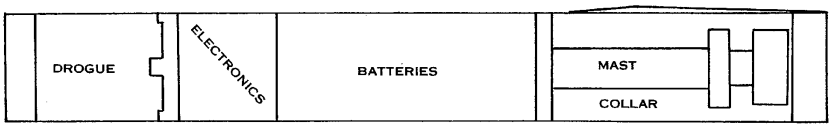

FIG. 2. Physical configuration of an AN/WSQ-6 acoustic drifter in a standard A-sized sonobuoy canister.

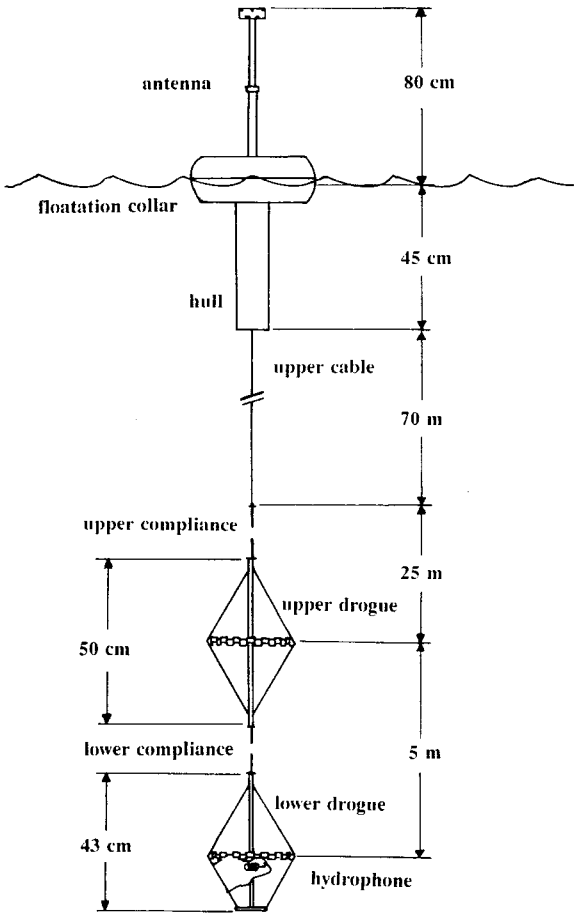

FIG. 3. Deployed configuration of an AN/WSQ-6 acoustic drifter.

contact with seawater, the seawater electrode triggers the gas cylinders to discharge, inflating the floatation collar, deploying the antenna and dropping the hydrophone package (hydrophone, drogues, weight, and cable). The physical configuration of a deployed buoy is shown in Fig. 3. Geophysical sensors include a hydrophone, thermistors, and a barometer.

The drogues are designed to decouple the motion of the surface buoy from the hydrophone, located at the lowest drogue. This is required to reduce flow noise, which would be detected as noise at frequencies below 100 Hz. The drogues produce a 17:1 drogue/cable to surface buoy drag ratio, thus providing limited Lagrangian drifter characteristics.

The pressure sensor is a low-cost, temperature compensated strain gauge with dynamic range 850–1054 mb ± 1 mb (McCormick et al. 1990). The pressure port, covered with a Gore-Tex splash guard, is at the top of the antenna mast to reduce problems with splash and submergence. The strain gauge itself is located at the bottom of the drifter hull, below the water line, to improve temperature stability.

The air temperature sensor, shielded from direct sun, is located near the top of the mast. It has a range of

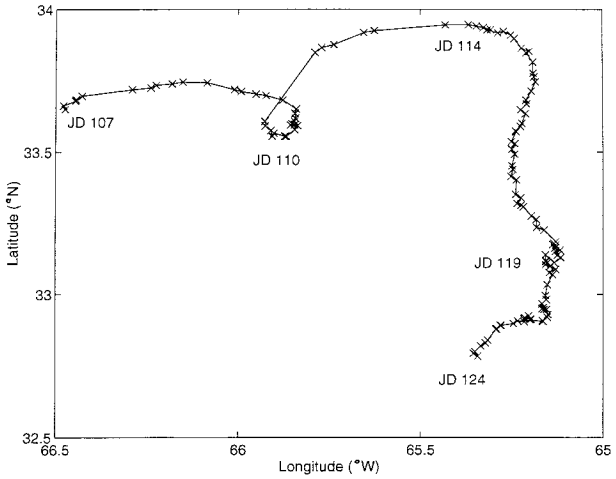

FIG. 4. Drifter 14 359 position in the North Atlantic from JD 107 to JD 136 1992.

−30° to 46°C ± 0.2°C. The surface water temperature sensor is incorporated into the base of the buoy hull. Its range and sensitivity is −5° to +35°C ± 0.2°C. Performance characteristics were verified by McCormick et al. (1990).

The ambient sound sensor is an omnidirectional (±1 dB below 10 kHz; ±3 dB from 10–25 kHz) hydrophone located at the lowest drogue at 100-m depth. The underwater sound field is sampled once per hour through 16 third octave band pass filters with center frequencies from 5 Hz to 25 kHz. The signal from each third octave filter is converted to a dc voltage using a root-mean-square circuit and is digitized using a 16-bit analog-digital circuit. The resulting dynamic range is nine orders of magnitude in acoustic intensity (35–125 dB ± 2 dB relative to 1 $mPa^2\ Hz^{-1}$ from 5 Hz to 5 kHz and 20–110 dB ± 2 dB relative to 1 $mPa^2\ Hz^{-1}$ from 8 to 25 kHz).

Data from the pressure, temperature, and ambient sound sensors are stored in six 32-bit data blocks and broadcast by the Argos satellite transmitter every 90 s. Depending on the buoy latitude, satellites are in position to receive the Argos transmission 8–12 times per day. The ambient noise data are sampled and updated once per hour, while data from the other sensors are sampled and updated every 10.5 min. Only the latest data are transmitted.

4. Example of data collection from an ANS drifter

On 16 April 1992 (Julian day or JD 106), an ANS drifter was deployed at 33.7°N, 66.4°W and reported data until JD 136. Figure 4 shows the drifter position during its lifetime. A strong atmospheric front passed over the drifter on JDs 119 and 120. The acoustic suspension system broke after this storm (on JD 122) and thereafter only surface sensor data (air, sea temperature, and barometric pressure data) were available. Figure 5

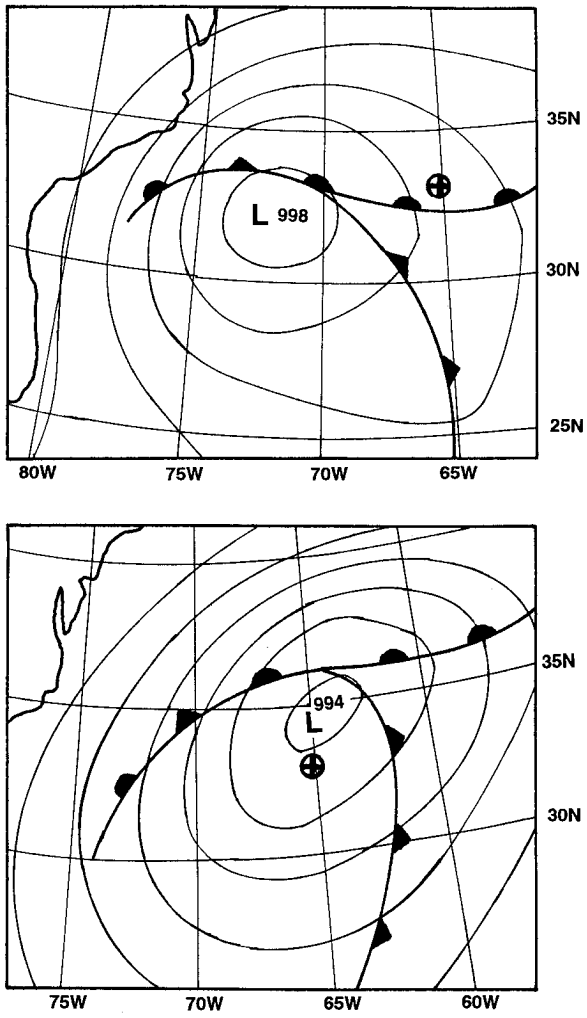

FIG. 5. Surface pressure charts for a storm passage over the drifter 14 359 on JD 119/120 1992.

shows surface pressure charts during the passage of the weather front on JD 119/120. Figure 6 shows the barometric pressure and temperature records from the drifter. The frontal passage is easily detected in the barometric pressure record and shows values consistent with the surface pressure charts. The air temperature record shows a diurnal heating pattern except during the frontal passage on JD 120. Note, in particular, the sudden drop in air temperature relative to sea surface temperature on JD 118 and JD 120. It will be argued that rain is acoustically detected at these times.

Figure 7 shows a time series of the underwater sound levels at seven frequencies between 50 and 25 000 Hz. In fact, 16 channels between 5 and 25 000 Hz were reported. Various acoustical ''events'' are indicated and will be discussed in more detail later. In general, the higher frequencies (over 500 Hz) are highly correlated with one another (correlation coefficients over 0.9). This is expected as the sound intensities at these frequencies

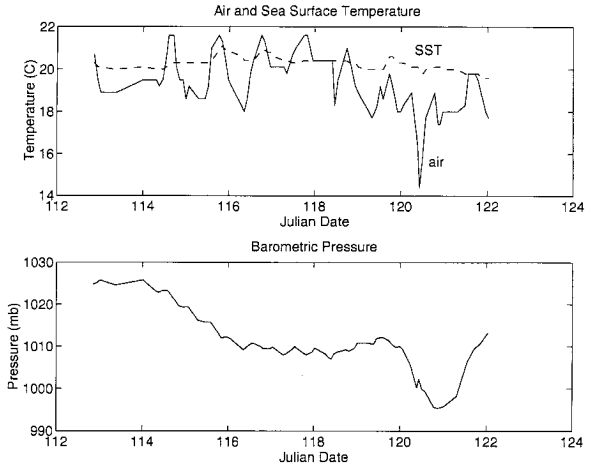

FIG. 6. Barometric surface pressure and temperature (air and sea) from drifter 14 359. Note the storm passage on JD 120.

are known to be correlated with wind speed. The events, attributed to nonwind processes, occur infrequently. It is assumed that wind-generated sound is ubiquitous. In the absence of nonwind events, the sound intensity level can be related to wind speed. Vagle et al. (1990) proposed an acoustic wind speed algorithm using the sound intensity at 8 kHz.

In contrast, the sound intensities between 10 and 100 Hz were found to be poorly correlated to each other and uncorrelated to the higher frequency channels. This is the spectral region where the ambient sound is attributed to ''distant shipping.'' Because of low acoustic attenuation in the ocean at these frequencies, long propagation paths from distant sources are possible. The low correlations suggest that the sound sources are narrow-

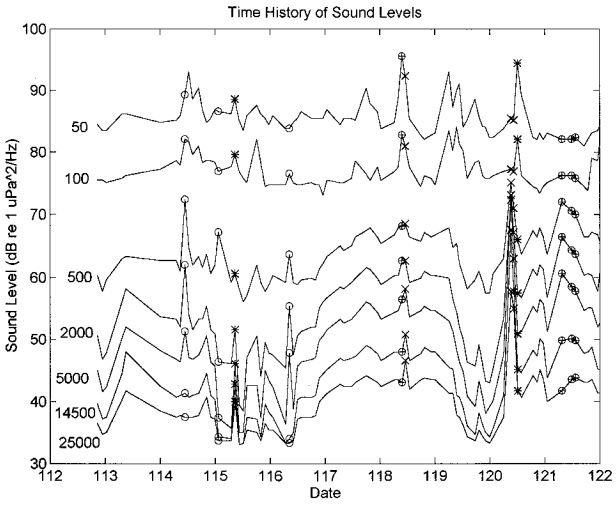

FIG. 7. Time series of sound intensity at selected frequencies. Nonwind events (shipping ''○,'' drizzle ''*,'' rain ''×,'' and high seas ''⊕'') are marked. These different events change the spectral character of the underwater sound field in predictable ways, allowing acoustic classification.

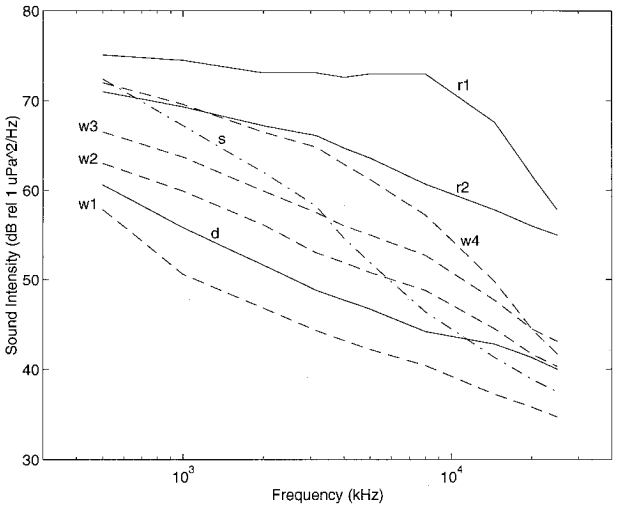

FIG. 8. Examples of sound spectra resulting in different weather classifications. The spectra labeled w1, w2, and w3 are ''wind only'' from JD 112.95, JD 113.3, and JD 117.95, respectively. Spectrum s is a probable ''shipping'' contamination from JD 114.45. Spectrum d is ''wind with drizzle'' from JD 115.36. Spectra r1 and r2 are ''heavy rain'' from JD 120.38 and JD 120.44, respectively. Spectrum w4 is classified as ''high seas'' and occurred at JD 121.31.

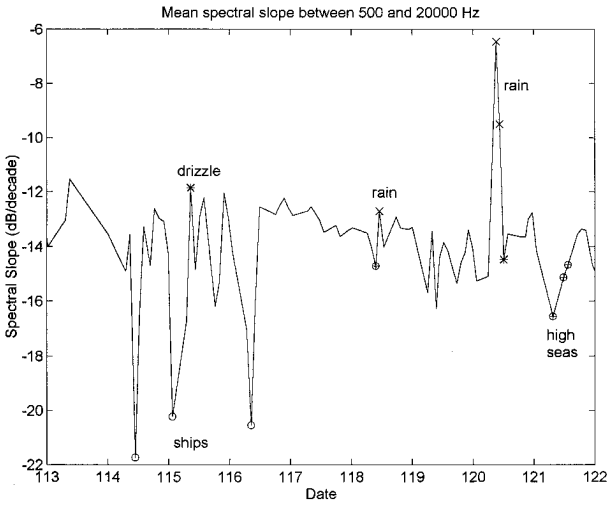

FIG. 9. Mean spectral slope between 500 Hz and 20 kHz for Drifter 14 359. Sound source identification for nonwind acoustical events (drizzle ''*,'' rain ''×,'' ships ''○,'' and high seas ''⊕'') are also indicated. The Vagle et al. (1990) value of −19 dB per decade for wind generated sound does not work for these data.

band in character and not related to local wind conditions. The sound field usually had a peak intensity near 50 Hz.

5. Data analysis—Interpretation of the ambient sound field

a. Algorithm to identify sound source (wind, rain, drizzle, and shipping)

Different underwater sound sources have different spectral shapes. These differences allow an algorithm to be designed to determine which process is dominating the sound field at a given time (the appendix). Four weather classifications are likely: wind only, wind with drizzle, heavy rain, and high seas. Examples of these classifications are shown in Fig. 8. In this discussion, the term ''high seas'' will refer to the modification of the sound field attributed to extensive ambient bubble clouds/layers, a distinct steepening of the spectral slope above 10 kHz. This type of modification to the sound field spectral shape has been observed during high wind (Farmer and Lemon 1984), changes of wind direction/speed during the passage of atmospheric fronts (Nystuen and Farmer 1989), and during heavy rain (Nystuen et al. 1993). Two spectra from Fig. 8 (r1 and w4) show this high-seas feature. Of course, it is expected that the sound field is occasionally contaminated by other sound sources. At specific locations or times, especially coastal locations, man-made or biological noise contamination may be persistent, for example, near ports or snapping shrimp beds. This does not appear to be a problem in deep ocean deployments.

One method of trying to identify spectral shape is to calculate a mean spectral slope and then compare it to the expected slope for wind speed (Vagle et al. 1990). The characteristic feature of the wind generated spectrum is the relatively uniform slope (see Fig. 8, spectra w1, w2, and w3). Vagle et al. (1990) reported a value of −19 dB per decade and proposed to detect ''wind'' when the observed slope was within ±3 dB per decade of this value. Figure 9 shows the spectral slope between 500 and 20 000 Hz for this ANS drifter. The mean value is −14 dB per decade, significantly different than the Vagle et al. value. The acoustic events from Fig. 7—shipping detection, rainfall, drizzle, and high seas—are again marked. Shipping is expected to ''redden'' the spectrum (see Fig. 8, spectrum s). Three spectra show this characteristic (JD 114.45, 115.06, and 116.35). While no independent verification of shipping is available, these spectra do represent anomalies from the expected sound field and should be considered ''contaminated.'' Rain is expected to ''whiten'' the spectrum. Two spectra show this characteristic (JD 120.38 and 120.44; Fig. 8, spectra r1 and r2, respectively). Independent confirmation of rainfall is available for these times. The rest of the spectra are within ±3 dB of the mean slope value and, consequently, would be classified as ''wind only'' using this type of spectral slope test. However, because the mean spectral slope is −14 dB per decade, strict application of the slope component of the Vagle et al. algorithm would classify almost all of these spectra as ''rain.'' Instead, it appears that the spectral slope varies, probably as a function of location and time. Dailey (1991) reported similar difficulty applying the −19 dB per decade mean and suggested that a running mean be defined and used to identify shipping or rainfall. In fact, the slope component of the Vagle et al.

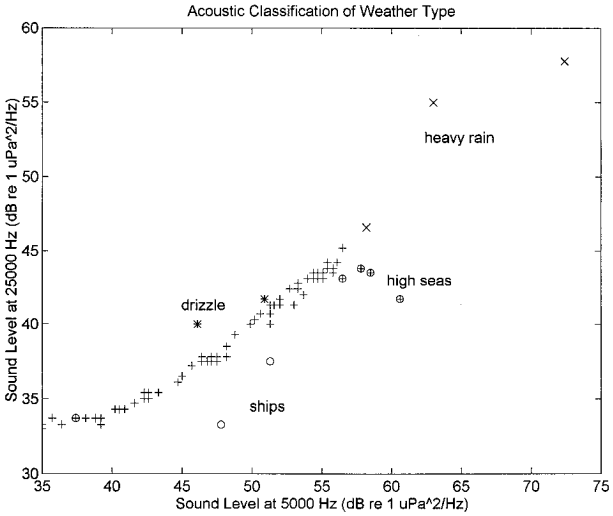

FIG. 10. A comparison of sound intensity at 5000 and 25 000 Hz for drifter 14 359. Detection of shipping ''○,'' high seas ''⊕,'' drizzle ''*,'' rain ''×,'' and wind-only ''+'' is accomplished by clustering of points on this type of figure.

algorithm is not used in the new classification algorithm described in the appendix.

The alternate method to obtain sound source classification is to compare the spectral levels at selected frequencies and use clustering to identify the sound source (Farmer and Lemon 1984). Figure 10 shows a comparison of spectral levels at 5 and 25 kHz. Most points fall along a fairly well-defined curve. These are assumed to be wind spectra, the most ubiquitous sound source. As the wind increases, wave breaking increases the sound intensity at both frequencies in a well-defined stretched S-shaped pattern. At the ''quiet'' end of these data points, the sound levels approach the background noise level for 25 kHz more quickly than at 5 kHz. Thus, the flattening of the curve. This feature is likely to be location dependent. At the ''loud'' end, bubble clouds attenuate the 25-kHz sound levels, but do not affect the sound at 5 kHz. Thus, as sea state increases, the sound at 5 kHz continues to increase but can actually decrease at 25 kHz (Farmer and Lemon 1984; compare spectra w3 and w4 from Fig. 8). This is because bubbles selectively attenuate sound at their resonance frequency. Few bubbles of the size needed to attenuate 5 kHz are present in the ambient bubble field (they are too big and float to the surface quickly), while many smaller bubbles (which attenuate higher frequencies) are present. Data points falling on this portion of the wind curve indicate high seas as many ambient bubbles, suggesting many breaking waves, must be present. Nonequilibrium wind–wave conditions, as well as very high wind speeds, could cause this to occur (Nystuen and Farmer 1989).

Other sound sources change the sound intensities in very different ways. For example, ships increase the low-frequency sound level more relative to the high-frequency channel. Thus, shipping is detected when data points fall below the wind curve. Drizzle produces excess sound at high frequencies and is therefore detected when data points fall above the wind curve. Heavy rain produces very loud levels at all frequencies and is detected by data points falling well above the curve, especially at higher frequencies (over 10 kHz). The dividing line between drizzle and heavy rain has not been well established but is important. When heavy rain is present, no estimate of wind speed is possible because the wind-generated sound (breaking waves) is overwhelmed by the rain sound. However, drizzle is observed to increase only the high-frequency (13 kHz and up) bands. Thus, drizzle detection does not preclude acoustical wind speed measurement. However, as drizzle turns to rain, the acoustical wind speed measurement will become contaminated.

b. Nonwind acoustical events

Several times during the data record, nonwind acoustical events are detected. The three shipping detections (JD 114.45, 115.06, and 116.35) have already been discussed. Each show excess sound levels at lower frequencies. Although two spectra show elevated levels as high as 5000 Hz, none show elevated levels at 14 500 Hz. The spectrum at 115.06 is odd, showing elevated levels only at 500 and 1000 Hz. While no independent verification of shipping is available, these spectra show anomalies that make them suspect. They are removed as ''contaminated.''

Ancillary geophysical data available to verify weather classification includes SSM/I satellite radiometer data and the air–sea temperature data on the buoy itself, plus the surface pressure field. The event on JD 118 (high seas at 118.40 and rain at 118.46) follows 10.8 h when the air and sea temperatures are the same, suggesting that the air–sea interface is ''well mixed,'' that is, high winds. When the rainfall is acoustically detected, the air temperature drops 2.1°C in 1.44 h. While certainly not definitive, a similar drop in air temperature relative to the sea surface temperature is present during the rainfall event on JD 120 and was usually present during other ''rainfall'' detections on other ANS drifter deployments. One potential explanation for this observation is evaporative cooling of the antenna mast on the buoy during rain.

The event on JD 120 (rain at JD 120.38, 120.44, and drizzle at JD 120.51) has collaborating SSM/I radiometer data (Fig. 11). The radiometer data are only 1 min (JD 120.38) prior to the acoustical record. Heavy rain is detected over the drifter location. During the rain, the relative drop in air temperature relative to the sea surface temperature is 4.4°C. Drizzle (at JD 120.51) immediately after rain is not unexpected. Confirmation of drizzle at sea is nearly impossible. A human observer is probably needed. Again, this spectra shows characteristics of the known effect of drizzle on the underwater sound field and so it should, at least, be flagged as

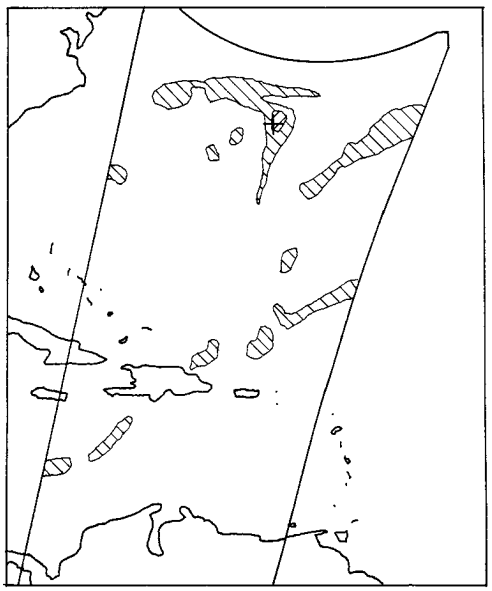

FIG. 11. The microwave (SSM/I) satellite image for rainfall rate 1 min prior (at 0913 UTC) to the acoustic rainfall detection (at 0914 UTC) at JD 120.38. The cross shows the buoy location. The shaded areas show rainfall rate over 1 mm h^{-1}. At the buoy location the rainfall rate is over 5 mm h^{-1}.

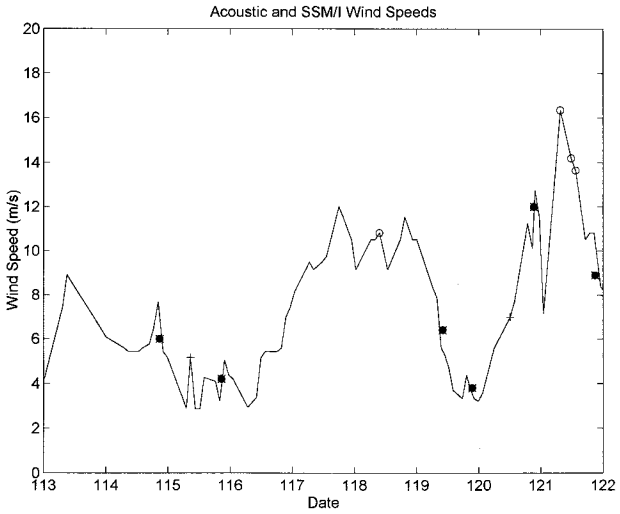

FIG. 12. A comparison of acoustically derived wind speeds from drifter 14359 and satellite derived wind speeds (SSM/I) at the drifter location (solid circles). The acoustic wind measurements with drizzle (cross) and high seas (open circle) are also indicated.

suspected drizzle. It is an anomaly from the typical wind only spectra.

The final event is high seas (JD 121.31, 121.49, and 121.56). High winds were recorded by the SSM/I radiometer after the passage of the storm. The air–sea temperature difference goes from −2.0°C to no temperature difference (the air temperature rises 1.8°C, while the sea surface temperature drops 0.2°C). This suggests active mixing of the near-surface water, consistent with wave breaking and bubble production.

c. Quantification of wind speed and rainfall rate

Once the sound source has been identified, quantification is possible. Two algorithms are presently available: wind speed (Vagle et al. 1990) and heavy rain (Nystuen et al. 1993). The algorithms are given in the appendix. The wind speed algorithm can be applied except when shipping or heavy rain are detected. These two sound sources obscure the sound from wind and, thus, make wind speed estimates impossible.

Figure 12 shows the acoustic wind speed estimates for drifter 14359. Comparison data are supplied by passive microwave satellite data from the DMSP SSM/I. The agreement is remarkably good. The passage of the front on JD 120 included a period of low wind, followed by relatively high winds and high sea states. The acoustic wind speed record has much better temporal resolution than the satellite data. At a specific location, satellite data are not available every day. Furthermore, for sun-synchronous satellites, the data are always recorded at the same local time. Of course, satellites provide large-scale spatial resolution.

ANS drifter wind speed data have been recorded for several other test deployments. The deployments were in the North Atlantic, North Pacific, and Gulf of Mexico. These data are combined in Fig. 13. The correlation between the acoustic and satellite wind speed estimates is $r = 0.91$. There is a tendency for the acoustic measurement to be biased low; however, there is not enough data to make a definitive statement. Dailey (1991) reported good agreement between acoustic and SSM/I wind speed estimates near the coast of California ($r =$

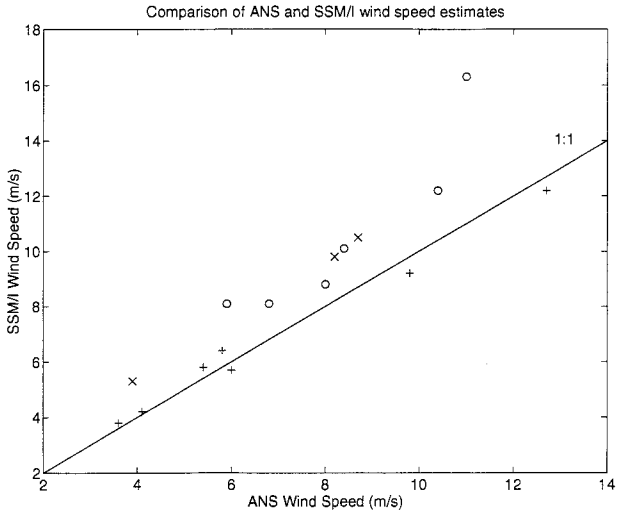

FIG. 13. Comparison of acoustically derived wind speeds and satellite wind speeds for several independent deployments of acoustic drifters. The deployments were in the North Pacific "○," North Atlantic "+," and Gulf of Mexico "×."

0.84). He also reported a bias toward low wind speed estimates for the acoustic method in warmer subtropical Pacific water.

Validation of rainfall rate measurements is even more difficult than for wind speed as there is no accepted method for making rainfall measurements at sea. The SSM/I radiometer does detect and attempt to quantify rainfall rate; however, verification of rainfall rate using the satellite data is extremely difficult for two reasons. First, collocated satellite passes are very infrequent and, second, quantitative estimates of rainfall rate from satellites are questionable. The rainfall detection at JD 120.38 was verified by a SSM/I satellite pass just one minute before the acoustic spectrum (Fig. 11). Heavy rain is indicated by the satellite, however, the value is only 5 mm h^{-1}. The acoustic estimate is 86 mm h^{-1}. This discrepancy is probably due to the relative spatial sampling characteristics of the two methods. For rainfall detection and measurement, the liabilities of the satellite are significant. Not only is the temporal sampling poor, the spatial footprint of the satellite is very large relative to the size of the rain cell. Thus, rainfall is inhomogeneous within the footprint of the satellite sensor. In contrast, for the acoustic drifters, the effective listening area for high-frequency sound is roughly 100 m in diameter centered over the hydrophone, a length scale smaller than most rain cells. An extremely heavy rainfall rate (86 mm h^{-1}) at the drifter's location is likely to be smoothed to a lower value when integrated over the satellite footprint.

6. Conclusions

Acoustic mini-drifting buoys have been developed to monitor upper-ocean air–sea interface processes in real time. These buoys are air-deployable standard sonobuoy-sized instruments. When deployed, a hydrophone is suspended below a small surface float. Data collected by the system are transmitted to users via the ARGOS satellite communication link. Atmospheric pressure, air and sea temperature, and ambient sound levels are measured directly. The ambient sound field can be further interpreted to measure wind speed, sea state, and precipitation.

Because of the different spectral character of the underwater sound produced by different air–sea processes, the sound field from 500 Hz to 25 kHz can be used to classify weather type. An algorithm used to identify the sound source (wind only, wind with drizzle, heavy rain, or shipping) is described and demonstrated using observations from a month-long deployment of a drifter in the North Atlantic. Various nonwind acoustic events are detected and are consistent with available ancillary data.

Acoustic measurements of wind speed and rainfall rate are possible for certain situations. The acoustic wind speed measurements are shown to be in excellent agreement with satellite wind speed estimates. The acoustic system has much higher temporal resolution than the satellite system. Rainfall detection is also demonstrated and compared to a satellite detection of heavy rain. The satellite measurement of rainfall rate is much lower than the acoustic measurement. This probably reflects the spatial sampling limitations of satellite rainfall quantification compared to the more localized acoustic measurement of rainfall rate.

Acknowledgments. This work was funded through the Oceanographer of the Navy's Center for Tactical Oceanographic Warfare Support program office at the Naval Research Laboratory, Code 7406, Stennis Space Center, MS, under the PE 0604218N R1740 drifting buoy project. Metocean Data Systems Ltd. of Dartmouth, Nova Scotia, Canada, developed and built the AN/WSQ-6 drifters.

APPENDIX

Algorithm for Weather Classification

The present algorithm relies on spectral shape differences to identify five categories of sound source: 1) shipping or other contamination, 2) heavy rain, 3) wind with drizzle, 4) wind only, and 5) high seas. It is based on data collected from an ANS drifter, number 14 359, deployed near Bermuda in April 1992. It is empirical. Most of the time, it is assumed that the sound field is generated by wind only processes. Various choices of frequencies were tried to identify times when ''unusual'' intensities were present. These were assumed to be generated by nonwind sources (rain, drizzle, high seas, and shipping). Evidence that these nonwind sources were present is verified or at least consistent with ancillary data.

The algorithm was verified using data from eight other ANS drifter deployments. In general, it worked well, although there is evidence of regional variation. In particular, five drifters deployed in the eastern North and equatorial Pacific recorded sound fields with steeper spectral slopes at frequencies over 10 kHz than those recorded by drifters in the western North Altantic, Gulf of Mexico, and western North Pacific. Consequently, for these drifters, the high-frequency sound intensities (at 20 or 25 kHz) were lower by 2–3 dB for a given lower frequency (1–5 kHz) sound intensity.

The algorithm consists of 1) a check for shipping or other low-frequency contamination, 2) a check for the high levels at higher frequencies associated with heavy rain, 3) a check for drizzle, and 4) a check for the attenuation of higher frequencies associated with high seas. If none of the checks is positive, then the sound source is assumed to be wind only. The spectral slope test of Vagle et al. (1990) is not used. Quantification of wind speed is possible for wind only, wind with drizzle, and high seas, although the wind speed algorithm of Vagle et al. (1990) is strictly valid only for the wind

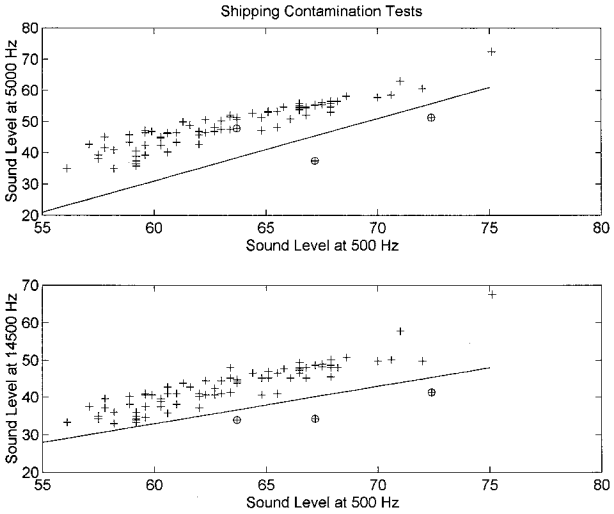

FIG. A1. Shipping detection test using 500, 5000, and 14 500 Hz.

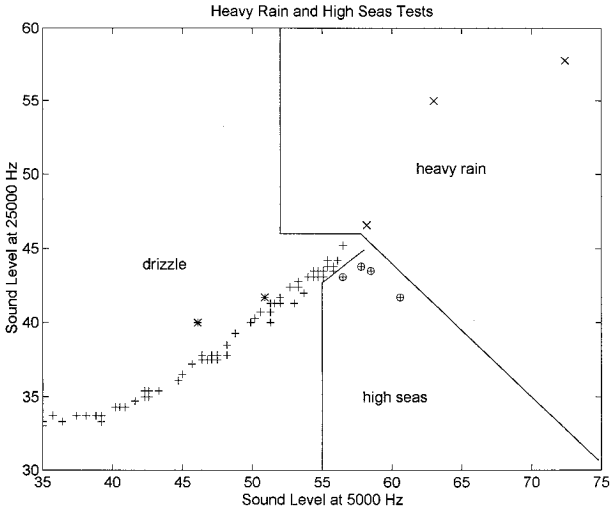

FIG. A2. Acoustic classification tests for rain and high seas.

only situation (for wind speeds of 2–15 m s^{-1} in absence of precipitation). Rainfall rate can also be quantified (Nystuen et al. 1993), although the algorithm was developed in a coastal environment and has not been verified in deep ocean situations. Drizzle should not be quantified as the sound source is a function of wind speed, although it can be assumed that the rainfall rate is not high (order 1 mm h^{-1}).

Step 1 is to check for excess low-frequency sound. The test is shown in Fig. A1. Frequencies used are 500, 5000, and 14 500 Hz. At 500 and 5000 Hz, there is no attenuation associated with bubbles (the high seas effect). Thus, sound levels associated with wind and rain are proportional to the wind speed or rainfall rate. The data shown are clustered, except for two points. These are assumed to be an indication of shipping contamination, as has been assumed in the past (i.e., Lemon et al. 1984). Low-frequency sound (at 500 Hz) can propagate from distant sources more readily as acoustic attenuation in the ocean is less for lower frequencies. Thus, a distant source should generate a sound field with excess low frequencies. At very least, these spectra are suspect and should be considered contaminated. Another test is shown in Fig. A1 using 500 and 14 500 Hz. The influence of frequency-dependent attenuation is even greater for these two frequency bands and a third suspicious spectrum is discovered. This point was not an anomaly in the first test as both the 500 and 5000 Hz intensities were elevated, possibly an indication of nearby shipping. If

$$2\,\mathrm{SPL}_{500} - \mathrm{SPL}_{5000} > 89,$$

or

$$\mathrm{SPL}_{500} > \mathrm{SPL}_{14\,500} + 27 \quad \text{and} \quad \mathrm{SPL}_{14\,500} < 40\ \mathrm{dB},$$

then shipping (or other) contamination is suspected; SPL_x is the sound pressure level (dB) relative to 1 $\mu\mathrm{Pa}^2$ Hz^{-1} at frequency x. The data point should not be further processed.

Step 2 is to check for high-frequency sound associated with heavy rain. Heavy rain produces extremely high sound intensities at all frequencies (above 500 Hz), especially above 20 kHz. In fact, very high wind processes do not produce sound intensities above 45 dB for frequencies over 20 kHz because of the attenuation associated with ambient bubbles (the high-seas effect). The frequencies used are 5000 and 25 000 Hz (Fig. A2). Three points are identified as heavy rain. The rainfall-rate algorithm of Nystuen et al. (1993) is only valid for sound intensities over 52 dB at 5000 Hz and thus the dividing line for drizzle for $\mathrm{SPL}_{5000} < 52$ dB. If

$$0.9\,\mathrm{SPL}_{5000} + \mathrm{SPL}_{25\,000} > 98 \text{ or } \mathrm{SPL}_{25\,000} > 46\ \mathrm{dB}$$

and

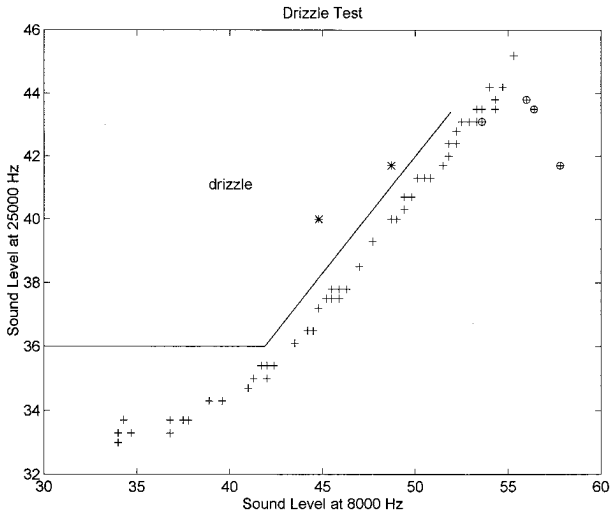

FIG. A3. Acoustic classification test for drizzle.

$$\mathrm{SPL}_{5000} > 52 \text{ dB},$$

then heavy rain is detected. The rainfall rate algorithm of Nystuen et al. (1993) can be applied to the data point. This algorithm is given by

$$\log_{10} R = \frac{\mathrm{SPL}_{5000} - 51.9}{10.6},$$

where R (mm h^{-1}) is rainfall rate. No further processing of the data is possible. The sound from heavy rain obscures the sound generated by other processes, in particular, wind associated sound.

Step 3 is to check for drizzle. Very light rain is observed to increase the sound level above 13 kHz due to the physical mechanism for sound production by small (1-mm diameter) raindrops. If only small raindrops are present (drizzle), then the lower frequencies (below 13 kHz) should not be affected by the drizzle. Figure A3 shows the comparison of 8000 and 25 000 Hz. Two points show excess high-frequency sound levels. Verification of drizzle present is difficult (confirmation only possible by human observer present?), however, these spectra do show the anomaly associated with drizzle and should be considered wind contaminated by drizzle. In theory, wind speed can be measured in the presence of drizzle, but as drizzle turns to rain, the wind speed measurement will become corrupted. Thus, wind speed calculated when drizzle is present should be flagged as less accurate (by overestimation) than the wind only category. Quantification of rainfall rate should not be attempted as the small drop sound production mechanism is sensitive to wind (Nystuen 1993). A rainfall rate of 1 mm h^{-1} is proposed as a generic ''light'' rainfall rate. If

$$0.74\ \mathrm{SPL}_{8000} - \mathrm{SPL}_{25\,000} < -5 \quad \text{and} \quad \mathrm{SPL}_{25\,000} > 36 \text{ dB},$$

then drizzle is present. The data can be further processed to measure wind speed, but a drizzle flag should be attached to the wind speed estimate. The rainfall rate can be set at 1 mm h^{-1}, a generic ''light'' rainfall rate.

Step 4 is to check for high seas. The term high seas refers to the change in the shape of the sound spectrum associated with high populations of bubbles in the water. This is assumed to be due to breaking waves from high winds (Farmer and Lemon 1984) or changing wind–wave sea conditions (Nystuen and Farmer 1989), thus the designation high seas. The high-frequency sound intensities are attenuated as small bubbles responsible for this attenuation are present in the water. Lower frequencies (5000 Hz and lower) are not affected as the bubbles required to attenuate the lower frequencies are too buoyant to remain in the water. Thus, it is thought that the lower frequencies continue to reflect increased breaking, and can still be used to measure wind speed. Note, however, that the Vagle et al. wind speed algorithm was developed using data for wind speeds up to 15 m s^{-1} and may not be accurate above 15 m s^{-1}. The test for high seas uses 5000 and 25 000 Hz and is shown in Fig. A2. If

$$0.74\ \mathrm{SPL}_{5000} - \mathrm{SPL}_{25\,000} > -2 \text{ and } \mathrm{SPL}_{5000} > 55 \text{ dB},$$

then high seas are present. Large populations of bubbles are suspected to be present. The Vagle et al. wind speed algorithm can be applied; however, a high-seas flag should be attached.

Step 5 is to apply the Vagle et al. (1990) wind speed algorithm. If shipping or heavy rain contamination is detected, the acoustical wind speed measurement is not valid and should not be attempted. If drizzle or high seas are detected, then the wind speed algorithm can be applied, but with caution (the points should be flagged). Otherwise, the wind speed algorithm can be applied. It is valid for wind speeds from 2 to 15 m $s^{-1} \pm 2$ m s^{-1}. Under 2 m s^{-1}, no wave (no wavelet) breaking occurs and thus there is no mechanism for wind to produce sound underwater. The algorithm was developed using wind speeds less than 15 m s^{-1}. While it may still be valid above 15 m s^{-1}, there is no verification of such performance and thus the error is unknown. The Vagle et al. (1990) wind speed algorithm is given by

$$U_{10} = \frac{10^{\mathrm{SPL}_{8000}/20} + 104.5}{53.91},$$

where U_{10} (m s^{-1}) is the 10-m wind speed.

REFERENCES

Dailey, C. H., 1991: Analysis of wind and rainfall measurements from acoustic drifters. M.S. thesis, Dept. of Oceanography, Naval Postgraduate School, 109 pp. [Available from Superintendent, Code 043, Naval Postgraduate School, Monterey, CA 93943-5000 or from Defense Technical Information Center, Cameron Station, Alexandria, VA 22304-6145.]

Evans, D. L., D. R. Watts, D. Halpern, and S. Bourassa, 1984: Oceanic winds measured from the seafloor. *J. Geophys. Res.*, **89,** 3457–3461.

Farmer, D. M., and D. D. Lemon, 1984: The influence of bubbles on ambient noise in the ocean at high wind speeds. *J. Phys. Oceanogr.*, **14,** 1762–1778.

——, and S. Vagle, 1988: On the determination of breaking wave distributions using ambient sound. *J. Geophys. Res.*, **93,** 3591–3600.

Franz, G., 1959: Splashes as sources of sound in liquids. *J. Acoust. Soc. Amer.*, **31,** 1080–1096.

Goodberlet, M. A., C. T. Swift, and J. C. Wilkerson, 1989: Remote sensing of ocean surface winds with the Special Sensor Microwave/Imager. *J. Geophys. Res.*, **94,** 14 547–14 555.

Heindsman, T. E., R. H. Smith, and A. D. Arneson, 1955: Effect of rain upon underwater noise levels. *J. Acoust. Soc. Amer.*, **27,** 378–379.

Knudsen, V. O., R. S. Alford, and J. W. Emling, 1948: Underwater ambient noise. *J. Mar. Res.*, **1,** 410–429.

Lemon, D. D., D. M. Farmer, and D. R. Watts, 1984: Acoustic measurements of wind speed and precipitation over a continental shelf. *J. Geophys. Res.*, **89,** 3462–3472.

Loewen, M. R., and W. K. Melville, 1994: An experimental investigation of the collective oscillations of bubble plumes entrained by breaking waves. *J. Acoust. Soc. Amer.*, **95,** 1329–1343.

McCormick, M. J., R. L. Pickett, and G. S. Miller, 1990: A field

evaluation of new satellite-tracked buoys: A LORAN-C position recording and a sonobuoy type drifter. *Marine Tech. Soc. J.*, **25,** 29–33.

Medwin, H., and M. M. Beaky, 1989: Bubble sources of the Knudsen sea noise spectra. *J. Acoust. Soc. Amer.*, **86,** 1124–1130.

——, J. A. Nystuen, P. W. Jacobus, D. E. Snyder, and L. H. Ostwald, 1992: The anatomy of underwater rain noise. *J. Acoust. Soc. Amer.*, **92,** 1613–1623.

Nystuen, J. A., 1993: An explanation of the sound generated by light rain in the presence of wind. *Natural Physical Sources of Underwater Sound*, B. R. Kerman, Ed., Kluwer Academic Publishers, 659–668.

——, 1996: Acoustical rainfall analysis: Rainfall drop size distribution using the underwater sound field. *J. Atmos. Oceanic Technol.*, **13,** 74–84.

——, and D. M. Farmer, 1987: The influence of wind of the underwater sound generated by light rain. *J. Acoust. Soc. Amer.*, **82,** 270–274.

——, and ——, 1989: Precipitation in the Canadian Atlantic Storms Program: Measurements of the acoustic signature. *Atmos.–Ocean*, **27,** 237–257.

——, and H. Medwin, 1995: Underwater sound generated by rainfall: Secondary splashes of aerosols. *J. Acoust. Soc. Amer.*, **97,** 1606–1613.

——, C. C. McGlothin, and M. S. Cook, 1993: The underwater sound generated by heavy precipitation. *J. Acoust. Soc. Amer.*, **93,** 3169–3177.

Pumphrey, H. C., L. A. Crum, and L. Bjorno, 1989: Underwater sound produced by individual drop impacts and rainfall. *J. Acoust. Soc. Amer.*, **85,** 1518–1526.

Scrimger, J. A., D. J. Evans, G. A. McBean, D. M. Farmer, and B. R. Kerman, 1987: Underwater noise due to rain, hail and snow. *J. Acoust. Soc. Amer.*, **81,** 79–86.

Selsor, H. D., 1993: Data from the sea: Navy Drifting Buoy Program. *Sea Technol.*, **34,** 53–58.

Shaw, P. T., D. R. Watts, and H. T. Rossby, 1978: On the estimation of oceanic wind speed and stress from ambient noise measurements. *Deep-Sea Res.*, **25,** 1225–1233.

Vagle, S., W. G. Large, and D. M. Farmer, 1990: An evaluation of the WOTAN technique for inferring oceanic winds from underwater sound. *J. Atmos. Oceanic Technol.*, **7,** 576–595.

Wenz, G. M., 1962: Acoustic ambient noise in the oceans: Spectra and sources. *J. Acoust. Soc. Amer.*, **34,** 1936–1956.